

Electronic inhomogeneities in the superconducting phase of $\text{CaFe}_{1.96}\text{Ni}_{0.04}\text{As}_2$ single crystals

Anirban Dutta¹, Neeraj Kumar², A. Thamizhavel², and Anjan K. Gupta¹

¹*Department of Physics, Indian Institute of Technology Kanpur, Kanpur 208016, India*

²*Department of Condensed Matter Physics and Materials Science,*

Tata Institute of Fundamental Research,

Homi Bhabha Road, Colaba, Mumbai 400 005, India

Abstract

Superconductivity in $\text{CaFe}_{2-x}\text{Ni}_x\text{As}_2$ emerges in close proximity to an antiferromagnetic (AFM) ordered parent state and the AFM phase overlaps with superconducting (SC) phase for a small range of x -values. We present scanning tunneling microscopy and spectroscopy study of an underdoped $\text{CaFe}_{2-x}\text{Ni}_x\text{As}_2$ single crystal in the vicinity of the boundary of the two phases. Both resistivity and magnetic susceptibility measurements show a superconducting T_C of 15 K and from later we deduce a superconducting fraction of 1.2 %. Topographic images show reasonably flat surface with signatures of atomic resolution. Spectra between 120 K and 20 K are spatially homogeneous and show signatures of spin density wave (SDW) gap. Below T_C , spectra show significant spatial inhomogeneity with a depression in density of states in ± 5 meV energy range. Inhomogeneity reduces significantly as the temperature goes above T_C and disappears completely far above T_C . These observations are discussed in terms of an inhomogeneous electronic phase that may exist due to the vicinity of this composition to the SC dome boundary on the underdoped side of the phase diagram.

I. INTRODUCTION

The superconductivity in Iron-Arsenic (Fe-As) based pnictides¹ emerges in close proximity to an AFM ordered parent state and T_C has dome-shaped dependence on doping or pressure²⁻¹³. In some pnictides, the AFM and SC phases overlap in the phase diagram and then the maximum T_C is found close to the extrapolated end point of the AFM transition. It is widely believed that magnetic fluctuations have an important role in the origin of high- T_C superconductivity. Quantum fluctuations associated with the quantum critical point (QCP)^{14,15} may also have a crucial role in superconductivity. Muon spin relaxation (μ SR) and Mössbauer spectroscopy on $\text{LaFeAsO}_{1-x}\text{F}_x$ show a discontinuous first-order-like transition from SDW to SC state without any coexistence of SDW and SC phases². Neutron scattering in $\text{CeFeAsO}_{1-x}\text{F}_x$ reveals a continuous second order transition, but the SDW and SC phases touch only at $T = 0$ and this could be a quantum critical point³. On the contrary, in other cases such as scanning tunneling microscopy and spectroscopy on $\text{NaFe}_{1-x}\text{Co}_x\text{As}$ ⁴, μ SR⁵⁻⁷ and neutron diffraction⁸ study on $\text{Ba}_{1-x}\text{K}_x\text{Fe}_2\text{As}_2$, μ SR study on $\text{Ba}(\text{Fe}_{1-x}\text{Co}_x)_2\text{As}_2$ ^{9,10} and on $\text{SmFeAsO}_{1-x}\text{F}_x$ ¹¹, μ SR and nuclear quadrupole resonance study on $\text{SmFe}_{1-x}\text{Ru}_x\text{AsO}_{0.85}\text{F}_{0.15}$ ¹² and ⁷⁵As NMR study on $\text{Ba}(\text{Fe}_{1-x}\text{Ru}_x)_2\text{As}_2$ ¹³ show coexistence of the two phases. These two phases may coexist microscopically or in a phase separated way. $\text{SmFe}_{1-x}\text{Ru}_x\text{AsO}_{0.85}\text{F}_{0.15}$ ¹² and $\text{Ba}(\text{Fe}_{1-x}\text{Ru}_x)_2\text{As}_2$ ¹³ display phase separation while $\text{NaFe}_{1-x}\text{Co}_x\text{As}$ ⁴, $\text{Ba}(\text{Fe}_{1-x}\text{Co}_x)_2\text{As}_2$ ^{9,10} show microscopic coexistence. In some pnictides for example $\text{Ba}_{1-x}\text{K}_x\text{Fe}_2\text{As}_2$ and $\text{SmFeAsO}_{1-x}\text{F}_x$, the issue of whether the two phases, AFM and SC, coexist microscopically or as phase separated, is not completely clear^{5-8,11}. With its atomic scale structural and spectroscopic imaging capabilities, scanning tunneling microscopy and spectroscopy (STM/S) is an ideal probe to investigate the local electronic properties of these systems. In our variable temperature STM/S we investigate the temperature evolution of the electronic density of states (DOS) to see how they correlate with various phases at different temperatures.

The parent compound CaFe_2As_2 undergoes a spin density wave (SDW) transition near $T_{SDW} = 170 \text{ K}$ ^{17,18}. Around T_{SDW} a structural transition is also observed, where the symmetry changes from tetragonal ($I4/mmm$) to orthorhombic ($Fmmm$)^{17,18}. Electron doping by partially replacing Fe by Ni suppresses the SDW and the structural transitions, leading to superconductivity in CaFe_2As_2 ¹⁹. With increase of Ni concentration, T_{SDW} starts to

decrease. Furthermore a drop in resistivity occurs at ~ 15 K for $x = 0.027$ which at higher doping develops into a pure superconducting transition¹⁹. SDW phase vanishes completely at $x = 0.06$ ¹⁹.

In this paper, we report temperature dependent STM/S studies of underdoped $\text{CaFe}_{1.96}\text{Ni}_{0.04}\text{As}_2$ single crystals in 5.4 K - 292 K temperature range. We observed flat terraces with some signatures of atomic resolution. Spectra show homogeneous tunneling DOS with SDW gap at high temperature and below T_C we see inhomogeneous local tunneling DOS with two kinds of spectra, either showing only SDW gap or a suppression in DOS in ± 5 mV bias range. Although these spectra below T_C are unlike those of typical SC, but the low energy DOS suppression is observed only below T_C . A preliminary version of this work was also reported by us in a conference²⁰.

II. EXPERIMENTAL DETAILS

Single crystals of $\text{CaFe}_{1.96}\text{Ni}_{0.04}\text{As}_2$ were grown¹⁹ by the high temperature solution growth using Sn-flux under identical conditions as mentioned in Ref.²¹. Electrical resistivity was measured using a standard four-probe method in a closed cycle refrigerator. DC magnetization was measured in a superconducting quantum interference device magnetometer. STM/S studies were done in cryogenic vacuum using a homemade variable temperature STM with fresh-cut $\text{Pt}_{0.8}\text{Ir}_{0.2}$ tips with RHK electronics and software. For STM/S measurements crystals were cleaved *in situ* at room temperature and at 4×10^{-6} mbar pressure before transferring the sample to the STM head at low temperature. Standard ac-modulation technique was used for STS measurements with a modulation amplitude between 1 and 10 mV and frequency 2731 Hz. For small bias (20 mV) we plot dI/dV directly to show the DOS, while we normalize the spectra for large bias (250 mV) to normalize away the effect of the tunnel matrix element on the spectra²². This process also sharpens the spectral features. We have seen similar results on 4-5 different samples of the same composition with more than one tip.

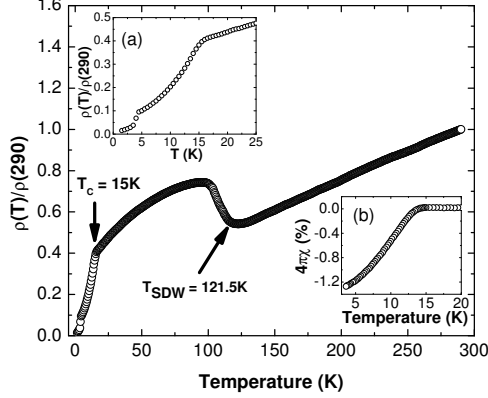


FIG. 1. Temperature dependence of the in plane electrical resistivity of a $\text{CaFe}_{1.96}\text{Ni}_{0.04}\text{As}_2$ single crystal. The inset (a) shows an expanded view of the region near the superconducting transition. The inset (b) shows temperature dependence of the zero field cooling (ZFC) magnetic susceptibility at 50 Oe.

III. RESULTS AND ANALYSIS

Fig. 1 shows the in-plane electrical resistivity of as-grown $\text{CaFe}_{1.96}\text{Ni}_{0.04}\text{As}_2$ single crystal. The in-plane resistivity decreases slowly with decreasing temperature below room temperature down to 121.5 K. Then there is a relatively broad upturn starting at $T_{SDW} = 121.5\text{K}$ due to SDW transition. This rise in resistivity is attributed to the opening of a gap in parts of the Fermi surface giving rise to a loss in DOS at E_F upon entering the SDW state. However, resistivity starts decreasing rapidly as the temperature is reduced further indicating that the Fermi surface is only partially gapped in the SDW state. As the temperature decreases further, a sharp drop in the resistivity occurs at $\sim 15\text{K}$ due to the onset of superconducting order. But the resistivity does not go to zero down to 1.3 K. Full superconducting transition develops only at slightly higher Ni doping (0.053 and 0.06)¹⁹ with an onset T_C of 15 K. The drop in the resistivity at $\sim 4\text{K}$ is due to the presence of traces of Sn, which is used as a flux. The inset (b) of Fig. 1 shows the temperature dependence of magnetic susceptibility χ measured under zero field cool (ZFC) condition at 50 Oe. Field was applied parallel to the ab -plane of the crystals. The susceptibility remains unchanged (nearly zero) with decreasing temperature down to 15 K. χ starts decreasing for temperature below $\sim 15\text{K}$ and becomes negative, but $4\pi\chi$ does not saturate down to 4 K. This indicates that the system is not fully shielded. Assuming demagnetization factor to be zero for $H \parallel ab$ -plane, measured shielding

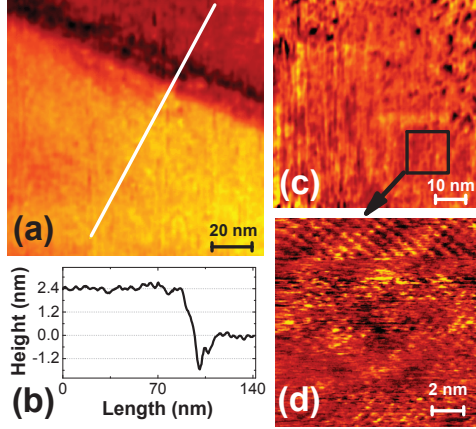


FIG. 2. (Color online) (a) STM topographic image (area: $140 \times 140 \text{ nm}^2$) of $\text{CaFe}_{1.96}\text{Ni}_{0.04}\text{As}_2$ single crystal at 292 K taken with a junction bias of 500 mV and a tunnel current of 60 pA. (b) Topographic profile along the lines marked in (a). (c) and (d) are the STM topographic images at 5.4 K of $69.22 \times 69.22 \text{ nm}^2$ and $13.17 \times 13.17 \text{ nm}^2$ respectively. Image in (c) was taken with a junction bias of 100 mV and a tunnel current of 100 pA while that in (d) was taken with constant height mode.

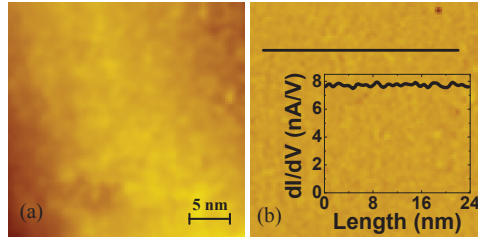


FIG. 3. (Color online) Simultaneously acquired (a) topographic and (b) conductance images (area: $29.03 \times 29.03 \text{ nm}^2$) of $\text{CaFe}_{1.96}\text{Ni}_{0.04}\text{As}_2$ single crystal at 110 K taken with a junction bias of 10 mV, a tunnel current of 100 pA and an ac-modulation voltage of 1 mV. The inset in (b) shows the dI/dV variation along the marked line, which is less than 2%.

fraction is only $\sim 1.2 \%$ at 5 K. Thus only a small portion of the system is superconducting at 4 K.

Fig. 2 show STM topographic images of *in situ* cleaved $\text{CaFe}_{1.96}\text{Ni}_{0.04}\text{As}_2$ single crystal at highest and lowest studied temperatures. Topographic image at 292 K (Fig. 2 (a)) show atomically flat surface over the terraces, with an rms roughness over any terrace as $\sim 0.11 \text{ nm}$. Similar kind of topographic images are observed at all studied temperatures. The line

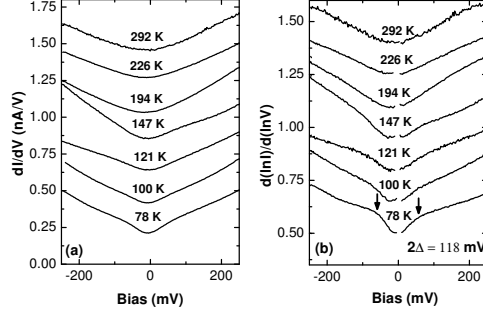


FIG. 4. Temperature dependent (a) dI/dV and (b) $d(\ln I)/d(\ln V)$ spectra of $\text{CaFe}_{1.96}\text{Ni}_{0.04}\text{As}_2$ single crystals between 292 K and 78 K. Spectra were taken with a junction bias of 250 mV, a tunnel current of 100 pA and an ac-modulation voltage of 10 mV. Consecutive spectra have been shifted uniformly upwards for clarity in all the three plots.

profile in Fig. 2 (b) shows that the terraces are separated by $\sim 2.4 (\pm 0.1)$ nm, i.e. twice the atomic steps¹⁹. Topographic images at the lowest studied temperature (5.4 K) are shown in Fig. 2 (c) and (d), which also show signatures of atomic resolution. Simultaneously acquired STM topographic and conductance images (area: 29.03×29.03 nm²) at 110 K are shown in Fig. 3. dI/dV along the marked line, in the conductance map as plotted in the inset, shows very little variation indicating an electronically homogeneous surface.

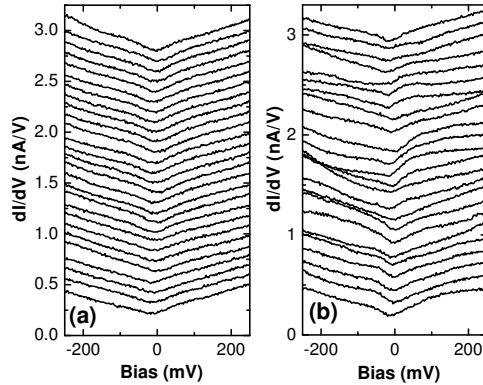


FIG. 5. dI/dV spectra of $\text{CaFe}_{1.96}\text{Ni}_{0.04}\text{As}_2$ single crystals taken at different locations of the sample at (a) 78 K and (b) 5.4 K. Spectra were taken with a junction bias of 250 mV, a tunnel current of 100 pA and an ac-modulation voltage of 10 mV. Consecutive spectra have been shifted uniformly upwards for clarity.

The temperature dependent tunneling spectra, dI/dV versus V between 78 K and 292 K are shown in Fig. 4 (a). Each plotted spectrum is a spatial average of about one hundred

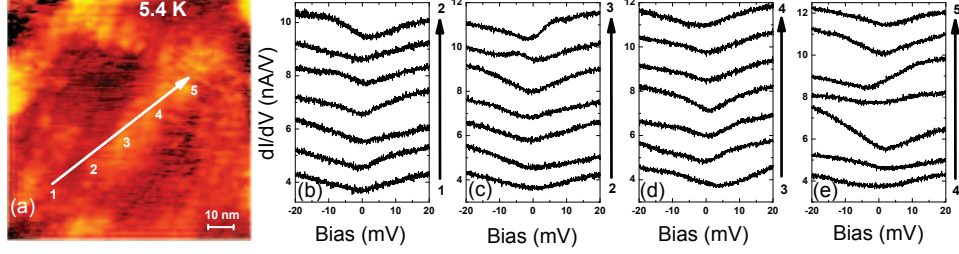


FIG. 6. (Color online) (a) STM topographic image at 5.4 K. (b)-(e) Spatially resolved dI/dV spectra along the marked line of the topographic image in (a). Separation between two consecutive spectra is 2.4 nm. Spectra were taken with a junction bias of 20 mV bias, a tunnel current of 100 pA and an ac-modulation voltage of 1 mV. Consecutive spectra have been shifted uniformly upwards for clarity in the plots (b)-(e).

spectra taken over an area of $\sim 2 \times 2 \mu\text{m}^2$, as they show very little variations (See Fig. 5 (a)). $d(\ln I)/d(\ln V) - V$ is plotted in Fig. 4 (b) which eliminates the effect of the voltage dependence of the tunneling matrix element and sharpens the gap feature²². Above T_{SDW} (121.5 K), there is a broad depression in the $d(\ln I)/d(\ln V) - V$ spectra which becomes more pronounced as the temperature goes below T_{SDW} . We attribute this to the opening of a partial gap at the E_F upon entering the SDW state. Similar kind of spectra were seen in EuFe_2As_2 ²². Local spectra at 78 K and 5.4 K, taken with same junction resistance and ac modulation are plotted in Fig. 5. We see significant spatial inhomogeneity at 5.4 K as compared to that at 78 K.

Spatially resolved dI/dV spectra along a line of a topographic image taken at 5.4 K are shown in Fig. 6. Each spectrum at a particular location is an average of 16 spectra and the distance between two consecutive locations is 2.4 nm. We clearly see that the nature of the spectra changes over nm length scale. To see the temperature evolution of these low energy features across the $T_C = 15$ K, we took $dI/dV - V$ spectra at different temperatures between 5.4 K and 20 K at different locations on the surface over an area of $\sim 2 \times 2 \mu\text{m}^2$. The spectra at 5.4 K and 19.7 K are shown in Fig. 7. We have grouped these spectra based on the symmetry of the features observed. None of the spectra show true superconducting gap with two coherence peaks but there is an asymmetric suppression in DOS in ± 5 mV bias range in some of the spectra. In some spectra, only one peak is observed near +5 mV in the dI/dV spectra. In some cases a sharp decrease in DOS occurs at negative bias without

any peak. Few spectra show a symmetric depression over ± 5 mV bias. In some locations the spectra show a rising DOS with a minima near zero bias but without any low energy features, i.e. these spectra are similar to the ones above 20 K.

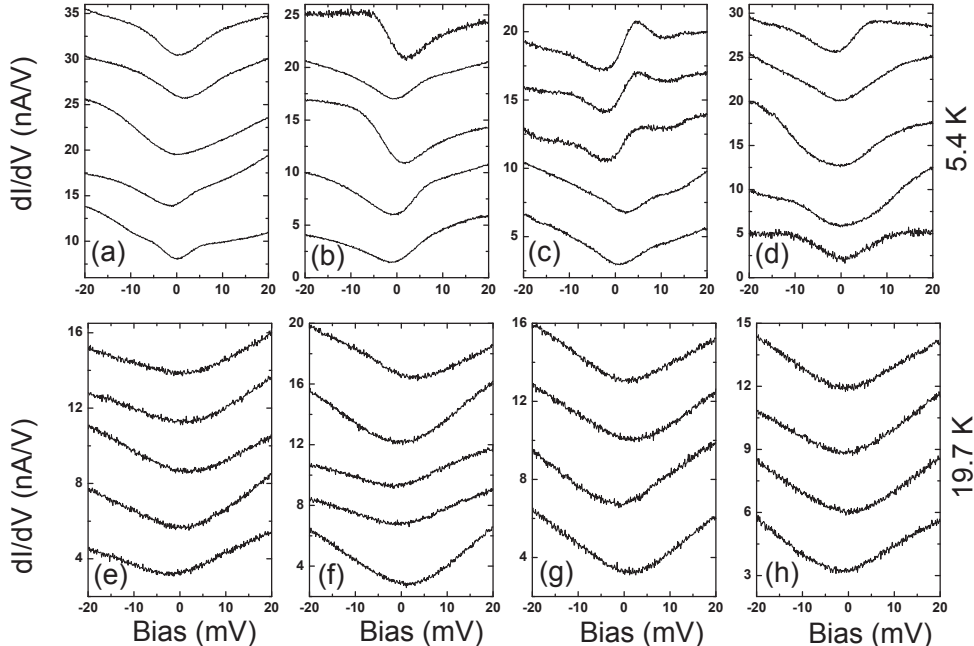


FIG. 7. (a)-(d) dI/dV spectra at different locations taken with a junction bias of 20 mV, a tunnel current of 100 pA and an ac-modulation voltage of 1 mV at 5.4 K. They have been grouped in different panels based on similarity between spectra. (e)-(h) dI/dV spectra at different locations taken with same parameters but at 19.7 K. Consecutive spectra have been shifted uniformly upwards for clarity in all the eight plots.

Based on the observed spectra at low temperature, we divided them into three categories: spectra with a sharp change in dI/dV at -ve bias, spectra with a peak at +ve bias, and spectra with no sharp change. We took the spatial average of the spectra showing peak at +ve bias and of those showing sharp change in DOS at -ve bias. We plot the temperature dependence of these two types of spatially averaged spectra in Fig. 8(a) and (b), which demonstrate the evolution of the DOS across T_C . Below T_C , there is some depression in the DOS near the Fermi energy (at zero bias) and this depression becomes more pronounced as the temperature goes down. We would like to state that we cannot track the same area as a function of temperature in our STM as the relative xy-shift between tip and sample with temperature is significant.

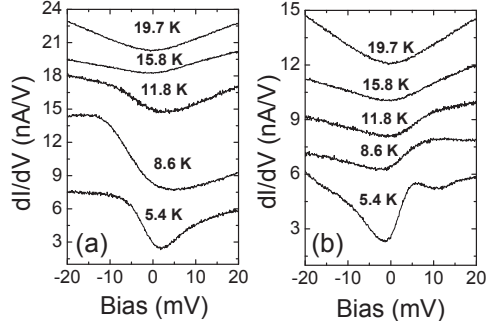


FIG. 8. (a) Spatially averaged dI/dV spectra with a sharp change in DOS at -ve bias at different temperatures and (b) Spatially averaged dI/dV spectra with a peak at +ve bias at different temperatures. Consecutive spectra have been shifted uniformly upwards in the two plots for clarity.

Our observed tunnel spectra at low temperatures are unlike those of typical superconductors, which show a BCS gap with two coherence peaks in DOS. However, the observed asymmetric or symmetric depression in DOS correlates well with the bulk superconductivity below T_C . Above T_C , there is no peak or depression in the low bias conductance but as the temperature reduces below the superconducting transition temperature, peak or depression in the tunnel spectra starts to appear. The depression in DOS at low energies is most pronounced at the lowest studied temperature. The temperature variation of the tunnel spectra across T_C clearly indicates that this peak disappears above superconducting transition. If we take a spatial average of these spectra we do get a gap-like structure with symmetric depression in DOS and weak peak-like features corresponding to BCS coherence peaks. Asymmetric spectra with gap have been seen routinely in high- T_C cuprates²³ with an energy gap and two coherence peaks. So the spectra that we observed are somewhat peculiar but the low energy asymmetric features are seen only below T_C .

IV. DISCUSSIONS

Emergence of inhomogeneous DOS only below the SC onset temperature is somewhat puzzling. It is possible that some small inhomogeneities do exist above T_C and they evolve into more clearly visible features below T_C . These features mainly involve an asymmetric depression in DOS near Fermi energy in 5 meV energy range. This energy scale is consistent with the typical superconducting gap reported in some of the pnictides^{4,24}. Susceptibility

data also show that a tiny fraction ($\sim 1.2\%$) of the system is in the SC state below T_C .

At low temperature tunnel spectra change significantly over a few nm length scale as seen in Fig. 6. A very homogeneous Ni distribution at this doping (0.04) will give ~ 1.4 nm average separation between Ni atoms in a-b plane. So we cannot reconcile our results with clustering of Ni atoms as that would lead to an inhomogeneity over a larger length scale. We have also seen the same inhomogeneous spectra in 4-5 different cleaved surfaces of these crystals, which makes it very unlikely that Ni is segregating over length scales larger than what is accessible to our STM. This is further ruled out from smooth susceptibility data without any sharp jumps. Signatures of atomic resolution and atomic steps with flat terraces make the surface contamination a very unlikely possibility.

It is possible that the cleaved surface differs from the bulk due to reconstruction, restructuring or other disorders²⁴. The nature of exposed surface after cleaving may depend on the cleaving temperature and a room temperature cleaving is more likely to yield a reconstructed surface. Moreover, a STM study²⁵ on $\text{Pr}_x\text{Ca}_{1-x}\text{Fe}_2\text{As}_2$ showed three different surface morphologies, 2×1 , 1×1 and a disordered web-like structure. Among these structures, 2×1 gives a non-polar surface while 1×1 gives a polar surface. In our atomic resolution images we saw only 1×1 structure at some places indicating a polar surface. Due to lack of atomic resolution over large area we cannot find the surface termination at various temperatures and locations to correlate with the local spectra. Masee et. al.²⁶, on room temperature cleaved $\text{BaFe}_{1.86}\text{Co}_{0.14}\text{As}_2$, showed that termination has little effect on the low-energy DOS. A hard X-ray photoemission also supports this finding²⁷. Thus we find it difficult to attribute the observed inhomogeneity over a few nm length-scale, in low-energy DOS and only below T_C , to the spatial variation in surface termination or reconstruction.

Inhomogeneities in tunnel conductance can also arise from quasi-particle interference (QPI) as reported in a STM study on doped CaFe_2As_2 ²⁸. In cuprates, spatially periodic DOS modulations have been seen over the SC gap energy scale due to QPI²⁹. More pronounced variations in local spectra of cuprates have been associated with oxygen inhomogeneities³⁰. In our spectra we see much wider spatial variations (see Fig. 6 and 7) than what is typically seen in QPI. We cannot rule out the QPI related inhomogeneities in present study, however we find it difficult to completely attribute these inhomogeneities to QPI.

In a typical pnictide phase diagram similar to cuprate superconductors, there is the famous superconducting dome and a phase boundary extending to much higher temperatures

that separates the SDW phase from the paramagnetic phase. Thus the phase boundaries touch the $T = 0$ axis at three points and it is not fully clear if all the three points are QCPs. The temperature dependent resistivity, penetration depth and spin-lattice relaxation measurements have strongly suggested that the point inside the dome is a QCP in pnictides^{14,15}. In cuprates, field doping near the first point (on underdoped side) has also revealed a QCP due to crossover between SC phase and an insulator phase³¹. Larger inhomogeneities have been observed in underdoped cuprates than the overdoped ones³². Superconductor to insulator transition has also been reported in heavily disordered conventional superconductors although it is not clear if this disorder also acts as a dopant and directly affects the SC order³³.

The composition of our crystals is close to the superconducting dome boundary on the underdoped side. Proximity to this boundary makes the non-SC phases easily accessible and presence of disorder will further help in nucleating such phases. We believe that in proximity to this crossover point, which may be a QCP, the system will be extremely susceptible to disorder and eventually the disorder might influence this crossover more than doping. Our results could be suggestive of the presence of a QCP at a point where the phase boundary touches the temperature axis in the underdoped side of pnictides.

V. CONCLUSIONS

In conclusion, our temperature dependent STM/S investigation of underdoped $\text{CaFe}_{1.96}\text{Ni}_{0.04}\text{As}_2$ single crystals show a highly inhomogeneous electronic phase below the SC transition temperature. At high temperatures we see a SDW gap consistent with the resistivity measurements. Magnetic measurement show that only a tiny fraction ($\sim 1.2\%$) of this compound superconducts below 15 K. Our STM measurements show atomically flat terraces with signatures of atomic resolutions at lowest temperature. Above T_C , the tunnel spectra show homogeneous local DOS with a SDW gap. But, below T_C , low energy scale spectra at some locations show an asymmetric or a symmetric dip in DOS at ± 5 meV energy, while, at other locations the spectra are similar to the ones at higher temperatures with SDW gap. This asymmetric or symmetric depression correlates well with the superconducting phase and the inhomogeneity disappears as the temperature goes above the superconducting transition temperature. Observed inhomogeneity over such a few nm length-scale and smooth

susceptibility data also exclude the possibility of segregation of Ni. From this STM/S study we believe that the inhomogeneities in this underdoped compound below T_C are intrinsic due to the proximity to the non-SC phase.

ACKNOWLEDGEMENTS

We thank Sourabh Barua for his help in the resistivity measurement. We also like to acknowledge Amit Dutta for helpful discussions. Anirban acknowledges financial support from the CSIR of the Government of India. A.K.G. acknowledges a research grant from the CSIR of the Government of India.

-
- ¹ Y. Kamihara, T. Watanabe, M. Hirano, and H. Hosono, *J. Am. Chem. Soc.* 130 (2008) 3296.
 - ² H. Luetkens et al., *Nature Mater.* 8 (2009) 305 .
 - ³ J. Zhao et al., *Nature Mater.* 7 (2008) 953.
 - ⁴ P. Cai et al., *Nat. Commun.* 4 (2013) 1596.
 - ⁵ T. Goko et al., *Phys. Rev. B* 80 (2009) 024508.
 - ⁶ J. T. Park et al., *Phys. Rev. Lett.* 102 (2009) 117006.
 - ⁷ E. Wiesenmayer, H. Luetkens, G. Pascua, R. Khasanov, A. Amato, H. Potts, B. Banusch, H. H. Klauss, and D. Johrendt, *Phys. Rev. Lett.* 107 (2011) 237001.
 - ⁸ H. Chen et al., *Europhys. Lett.* 85 (2009) 17006.
 - ⁹ P. Marsik et al., *Phys. Rev. Lett.* 105 (2010) 057001.
 - ¹⁰ C. Bernhard et al., *Phys. Rev. B* 86 (2012) 184509.
 - ¹¹ A. J. Drew et al., *Nature Mater.* 8 (2009) 310.
 - ¹² S. Sanna, P. Carretta, P. Bonfà, G. Prando, G. Allodi, R. De Renzi, T. Shiroka, G. Lamura, A. Mårtinelli, and M. Putti, *Phys. Rev. Lett.* 107 (2011) 227003.
 - ¹³ Y. Laplace, J. Bobroff, V. Brouet, G. Collin, F. Rullier-Albenque, D. Colson, and A. Forget, *Phys. Rev. B* 86 (2012) 020510(R).
 - ¹⁴ R. Zhou, Z. Li, J. Yang, D. L. Sun, C. T. Lin and Guo-qing Zheng, *Nat. Commun.* 4 (2013) 2265.
 - ¹⁵ T. Shibauchi, A. Carrington and Y. Matsuda, *Annu. Rev. Condens. Matter Phys.* 5 (2014) 113.

- ¹⁶ M. H. Julien, H. Mayaffre, M. Horvatić, C. Berthier, X. D. Zhang, W. Wu, G. F. Chen, N. L. Wang, and J. L. Luo, *Euro. Phys. Lett.* 87 (2009) 37001.
- ¹⁷ N. Ni, S. Nandi, A. Kreyssig, A. I. Goldman, E. D. Mun, S. L. Bud'ko, and P. C. Canfield, *Phys. Rev. B* 78 (2008) 014523.
- ¹⁸ F Ronning, T Klimczuk, E D Bauer, H Volz and J D Thompson, *J. Phys.: Condens. Matter* 20 (2008) 322201.
- ¹⁹ N. Kumar, Songxue Chi, Ying Chen, Kumari Gaurav Rana, A. K. Nigam, A. Thamizhavel, William Ratcliff, II, S. K. Dhar, and Jeffrey W. Lynn, *Phys. Rev. B* 80 (2009) 144524.
- ²⁰ A. Dutta, A. Thamizhavel, and A. K. Gupta, *AIP Conference Proceedings* 1591 (2014) 1657.
- ²¹ N. Kumar, R. Nagalakshmi, R. Kulkarni, P. L. Paulose, A. K. Nigam, S. K. Dhar, and A. Thamizhavel, *Phys. Rev. B* 79 (2009) 012504.
- ²² A. Dutta, Anupam, Z. Hossain and A. K. Gupta, *J. Phys.: Condens. Matter* 25 (2013) 375602.
- ²³ S. H. Pan et. al., *Nature* 413 (2001) 282.
- ²⁴ Jennifer E Hoffman, *Rep. Prog. Phys.* 74, (2011) 124513.
- ²⁵ Ilija Zeljkovic, Dennis Huang, Can-Li Song, Bing Lv, Ching-Wu Chu, and Jennifer E. Hoffman, *Phys. Rev. B* 87 (2013) 201108(R).
- ²⁶ F. Masee, Y. Huang, R. Huisman, S. de Jong, J. B. Goedkoop, and M. S. Golden, *Phys. Rev. B* 79 (2009) 220517(R).
- ²⁷ S. de Jong, Y. Huang, R. Huisman, F. Masee, S. Thirupathaiiah, M. Gorgoi, F. Schaefer, R. Follath, J. B. Goedkoop, and M. S. Golden, *Phys. Rev. B* 79 (2009) 115125.
- ²⁸ T.-M. Chuang, M. P. Allan, Jinho Lee, Yang Xie, Ni Ni, S. L. Budko, G. S. Boebinger, P. C. Canfield, and J. C. Davis, *Science* 327, (2010) 181.
- ²⁹ J. E. Hoffman, K. McElroy, D.-H. Lee, K. M. Lang, H. Eisaki, S. Uchida, and J. C. Davis, *Science* 297 (2002) 1148.
- ³⁰ K. McElroy, Jinho Lee, J. A. Slezak, D.-H. Lee, H. Eisaki, S. Uchida, J. C. Davis, *Science* 309 (2005) 1048.
- ³¹ A. T. Bollinger, G. Dubuis, J. Yoon, D. Pavuna, J. Misewich, and I. Božović, *Nature* 472 (2011) 458.
- ³² K. K. Gomes, A. N. Pasupathy, A. Pushp, S. Ono, Y. Ando, and A. Yazdani *Nature* 447 (2007) 569.
- ³³ A. M. Goldman, and N. Markovic, *Phys. Today* 51 (1998) 39.